

# Magnetic ordering in a doped frustrated spin-Peierls system

Nicolas Laflorencie,<sup>1</sup> Didier Poilblanc,<sup>2</sup> and Anders W. Sandvik<sup>3</sup>

<sup>1</sup>*Laboratoire de Physique Théorique, CNRS-UMR5152 Université Paul Sabatier, F-31062 Toulouse, France*

<sup>2</sup>*Laboratoire de Physique Théorique (CNRS-UMR5152),  
Université Paul Sabatier, F-31062 Toulouse, France*

<sup>3</sup>*Department of Physics, Åbo Akademi University, Porthansgatan 3, FIN-20500 Turku, Finland*

(Dated: November 2, 2018)

Based on a model of a quasi-one dimensional spin-Peierls system doped with non-magnetic impurities, an effective two-dimensional Hamiltonian of randomly distributed  $S=1/2$  spins interacting via long-range pair-wise interaction is studied using a stochastic series expansion quantum Monte Carlo method. The susceptibility shows Curie-like behavior at the lowest temperatures reached although the staggered magnetisation is found to be finite for  $T \rightarrow 0$ . The doping dependance of the corresponding three-dimensional Néel temperature is also computed.

PACS numbers: 75.10.-b 71.27.+a 75.50.Ee 75.40.Mg

Quasi one-dimensional (1D) quantum antiferromagnets exhibit fascinating magnetic properties at low temperatures. Some inorganic compounds, such as the germanate oxide  $\text{CuGeO}_3$ <sup>1</sup> and the vanadate oxide  $\text{LiV}_2\text{O}_5$ <sup>2</sup> are excellent realizations of weakly interacting frustrated spin-1/2 chains. A spin-Peierls (SP) transition to a gapped dimerised ground state (GS) has been seen experimentally in  $\text{CuGeO}_3$ <sup>1</sup>, and theoretical calculations<sup>3</sup> point toward a similar scenario in  $\text{LiV}_2\text{O}_5$ . Doping with non-magnetic dopants is realized experimentally in  $\text{CuGeO}_3$  by substituting a small fraction of copper atoms by zinc (or magnesium) atoms<sup>4</sup>. An intriguing low-temperature phase where antiferromagnetism coexists with the SP dimerisation was observed<sup>4</sup>. Similar doping-induced antiferromagnetic (AF) ordering has also been observed in the interacting dimer compound  $\text{TlCuCl}_3$ <sup>5</sup>. Theoretically, each dopant is expected to release a soliton which can be viewed as a single unpaired spin separating two dimer configurations<sup>6</sup>, hence leading to a rapid suppression of the spin gap under doping<sup>7</sup>. In an idealized *spontaneously* dimerised spin chain the soliton would not be bound to the dopant<sup>6</sup>. The physical picture is in fact completely different: A static *bulk* dimerisation is enforced by, e.g., couplings to the three-dimensional (3D) lattice, thus generating an attractive potential between the soliton and the dopant<sup>6,8</sup>.

The dopant-soliton confinement mechanism is responsible for the formation of local  $S=1/2$  magnetic moments<sup>6,9</sup>. Within a realistic model including an elastic coupling to a two-dimensional (2D) lattice<sup>10</sup>, it was shown that these effective spins experience a non-frustrated interaction that could lead at  $T = 0$  to a finite staggered magnetization<sup>11</sup>. Recently, similar conclusions were reached using a model with purely magnetic interactions including a four-spin exchange coupling<sup>12</sup>. In this Letter, we analyze the formation of the dopant-induced AF order which coexists with the SP dimerisation. After using exact diagonalisation (ED) of small clusters (following Refs.<sup>11,12</sup>) to construct an effective diluted  $S=1/2$  model, we take advantage of the non-frustrated character of the resulting Hamiltonian to perform extensive

state-of-the-art stochastic series expansion (SSE) quantum Monte Carlo (QMC) simulations on 2D lattices as large as  $288 \times 288$  with up to  $N_s = 576$  (dopant) spins and down to temperature as low as  $T = 1/\beta = 2^{-14}$  (or  $2^{-18}$  for  $N_s = 256$ ). The uniform susceptibility is shown to exhibit a Curie-like behavior although the  $T = 0$  and infinite size extrapolated staggered magnetization is found to be finite down to the smallest dopant concentrations  $x$  available. The Néel temperature (assuming a small 3D coupling) is also computed versus  $x$  and compared to experiments.

We start with the microscopic Hamiltonian of a 2D array of coupled frustrated spin- $\frac{1}{2}$  chains and we summarize the procedure followed in refs.<sup>11,12</sup> to derive an effective Hamiltonian.

$$H = \sum_{i,a} [J(1 + \delta_{i,a}) \mathbf{S}_{i,a} \cdot \mathbf{S}_{i+1,a} + \alpha J \mathbf{S}_{i,a} \cdot \mathbf{S}_{i+2,a} + h_{i,a} S_{i,a}^z], \quad (1)$$

where the  $i$  and  $a$  indices label the  $L$  sites and  $M$  chains respectively. The energy scale is set by the exchange coupling along the chain ( $J = 1$ ) and  $\alpha$  is the relative magnitude of the next nearest neighbor frustrating magnetic coupling. Dopants are simply described as randomly located inert sites ( $i, a$ ) (see Fig. 1) where  $\mathbf{S}_{i,a} = \mathbf{0}$  is set in Eq. (1). Small inter-chain couplings are included in a mean-field self-consistent treatment assuming,

$$h_{i,a} = J_{\perp} (\langle S_{i,a+1}^z \rangle + \langle S_{i,a-1}^z \rangle), \quad (2)$$

$$\delta_{i,a} = \frac{J_4}{J} \{ \langle \mathbf{S}_{i,a+1} \cdot \mathbf{S}_{i+1,a+1} \rangle + \langle \mathbf{S}_{i,a-1} \cdot \mathbf{S}_{i+1,a-1} \rangle \} \quad (3)$$

While the first term accounts for first-order effects in the inter-chain magnetic coupling  $J_{\perp}$ , the second term might have multiple origins; although a four-spin cyclic exchange mechanism provides the most straightforward derivation of it<sup>12</sup>, at a qualitative level,  $J_4$  can also mimic higher-order effects in  $J_{\perp}$ <sup>13</sup> or the coupling to a 2D (or 3D) lattice. In that case, due to a magneto-elastic coupling, the modulations  $\delta_{i,a}$  result from small displacements of the ions. The elastic energy is the sum of a

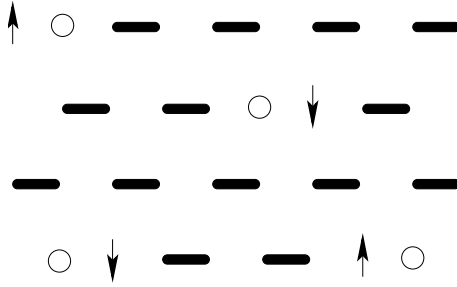


FIG. 1: Schematic picture of a doped SP system. Thick bonds correspond to dimers, and non-magnetic dopants (released spin- $\frac{1}{2}$ ) are represented by open circles (arrows).

local term  $\frac{1}{2}K_{\parallel}\sum_{i,a}\delta_{i,a}^2$  and an inter-chain contribution  $K_{\perp}\sum_{i,a}\delta_{i,a}\delta_{i,a+1}$  of electrostatic origin<sup>14</sup>. In that case Eq. (3) is replaced by<sup>10</sup>,  $K_{\parallel}\delta_{i,a} + K_{\perp}(\delta_{i,a+1} + \delta_{i,a-1}) = J\langle\mathbf{S}_{i,a} \cdot \mathbf{S}_{i+1,a}\rangle$ , giving very similar results<sup>15</sup> so that we shall restrict to Eq. (3) here.

By breaking a dimer, each dopant releases a soliton carrying a spin 1/2. As shown previously<sup>12</sup>,  $J_4$  (or equivalently  $K_{\perp}$  in the alternative model<sup>10</sup>) leads to a confinement of the moment to the dopant with a localization length  $\sim J_4^{-\eta}$ . At temperatures lower than the spin gap, these effective spins dominate the physics (see Fig.1) and a low-temperature description of the doped system can be obtained using an effective model including only (long-range) pair-wise interaction between these local moments. The coupling  $J^{\text{eff}}$  between two effective spins at arbitrary relative distance is computed by ED as the energy difference between their singlet and triplet configurations<sup>11,12</sup>. The sign of this interaction (i.e. its ferromagnetic or AF nature) depends on whether the two dopants lie on the same or opposite sublattices<sup>16</sup>, so that an overall AF ordering is favored.

In order to derive an analytic expression for  $J^{\text{eff}}$  valid at long distances, we fit the numerical ED data (restricted to short and intermediate length scales). A long-range *non-frustrated* Heisenberg model of diluted effective spin- $\frac{1}{2}$  can then be defined,

$$\mathcal{H}^{\text{eff}} = \sum_{\mathbf{r}_1, \mathbf{r}_2} \epsilon_{\mathbf{r}_1} \epsilon_{\mathbf{r}_2} J^{\text{eff}}(\mathbf{r}_1 - \mathbf{r}_2) \mathbf{S}_{\mathbf{r}_1} \cdot \mathbf{S}_{\mathbf{r}_2}, \quad (4)$$

with  $\epsilon_{\mathbf{r}} = 1$  (0) with probability  $x$  ( $1 - x$ ), where  $x$  is the dopant concentration. Such a model can be studied by QMC on  $L_x \times L_y$  clusters much larger than those accessible to ED<sup>11</sup> and *at all temperatures*. Using five phenomenological parameters, two energy scales and three length scales, simple expressions fit the ED data for a wide range of (physical) parameters. Naturally, one has to distinguish four cases depending on whether the dopants are located on the same ( $\Delta a = 0$ ) or on different chains, and whether they are located on the same or on different sublattices. When  $\Delta a = 0$  (same chain),  $J^{\text{eff}}$  approximately fulfills  $J^{\text{eff}}(\Delta i, 0) =$

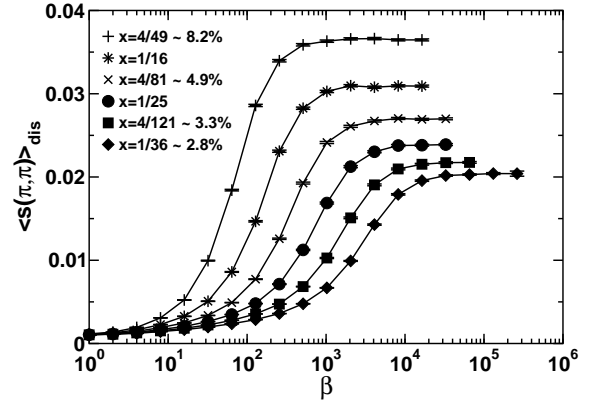


FIG. 2: Staggered magnetic structure factor per site vs inverse-temperature  $\beta$  computed using a  $\beta$ -doubling scheme and averaged over 1000 to 2000 samples. Results for  $N_s = 256$  spins on  $56 \times 56$ ,  $64 \times 64$ ,  $72 \times 72$ ,  $80 \times 80$ ,  $88 \times 88$  and  $96 \times 96$  (from top to bottom) lattices correspond to the concentrations  $x$  indicated on the plot.

$J_0(1 - \Delta i/\xi_{\parallel}^0)$  for  $\Delta i$  even and  $\Delta i < \xi_{\parallel}^0$  and otherwise  $J^{\text{eff}}(\Delta i, 0) = 0$ . For dopants located on different chains and on the same sublattice ( $\Delta i + \Delta a$  even) one has,  $J^{\text{eff}}(\Delta i, \Delta a) = -J'_0 \exp(-\frac{\Delta i}{\xi_{\parallel}}) \exp(-\frac{\Delta a}{\xi_{\perp}})$ , while, if the dopants are on opposite sublattices,  $J^{\text{eff}}(\Delta i, \Delta a) = J'_0 \frac{\Delta i}{2\xi_{\parallel}} \exp(-\frac{\Delta a}{\xi_{\perp}})$  for  $\Delta i \leq 2\xi_{\parallel}$  and  $J^{\text{eff}}(\Delta i, \Delta a) = J'_0 \exp(-\frac{\Delta i - 2\xi_{\parallel}}{\xi_{\parallel}}) \exp(-\frac{\Delta a}{\xi_{\perp}})$ , for  $\Delta i > 2\xi_{\parallel}$ . The fitting parameters used here for  $\alpha = 0.5$ ,  $J_{\perp} = 0.1$  and  $J_4 = 0.08$  are  $J_0 = 0.52$ ,  $J'_0 = 0.3$ ,  $\xi_{\parallel}^0 = 17.3$ ,  $\xi_{\parallel} = 2.5$  and  $\xi_{\perp} = 1$ . We stress that the alternating sign of  $J^{\text{eff}}$  is a crucial feature of the interaction which guarantees the absence of frustration. Note also that the magnitude of  $J^{\text{eff}}$  shows a unique exponential behavior  $\propto \exp(-\frac{\Delta i}{\xi_{\parallel}} - \frac{\Delta a}{\xi_{\perp}})$  at long distance although its short distance behavior is more complicated (but probably not relevant). The distribution of these coupling contains a very large density of couplings of small magnitudes.

We study the effective Heisenberg model using the SSE method<sup>17</sup> to investigate GS as well as finite  $T$  properties. In this approach, the interactions are sampled stochastically, and for a long-ranged interaction the computational effort is then reduced from  $\sim N_s^2$  to  $N_s \ln(N_s)$ <sup>18</sup>. In order to accelerate the convergence of the simulations at the very low temperatures needed to study the ground state, we use a  $\beta$ -doubling scheme<sup>19</sup> where the inverse temperature is successively increased by a factor 2. Comparing results at several  $\beta = 2^n$ , one can subsequently check that the  $T \rightarrow 0$  limit has been reached.

The AF ordering instability is signalled by the divergence with system size of the staggered structure factor,

$$S(\pi, \pi) = \frac{1}{L_x L_y} \langle \left( \sum_i (-1)^i S_i^z \right)^2 \rangle. \quad (5)$$

Note that within our effective model approach, only the

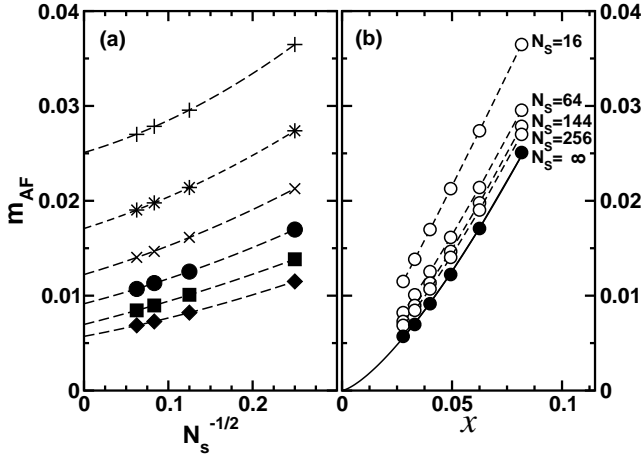


FIG. 3: Staggered magnetization per site. Disorder average has been done over at least 2000 samples. (a) Finite size extrapolations (see text) at fixed doping  $x$ . The symbols are identical to Fig.2 for  $x$  varying from  $\sim 2.8\%$  to  $\sim 8.2\%$ . (b) Doping dependance of  $m_{AF}$  for various numbers of spins and in the thermodynamic limit (full symbols).

sites carrying a "dopant spin" contribute to this sum. It is convenient to normalize  $S$  with respect to the number of sites, i.e. to define a staggered structure factor per site;  $s(\pi, \pi) = S(\pi, \pi)/L_x L_y$ . In an ordered AF state,  $s(\pi, \pi)$  should converge, with increasing size, to a non-zero value  $< 1/4$ . The (finite size) sublattice magnetization  $m_{AF}$  can then be obtained by averaging  $s(\pi, \pi)$  over a large number of dopant distributions, i.e.  $(m_{AF})^2 = 3\langle s(\pi, \pi) \rangle_{\text{dis}}$ , where the factor 3 comes from the spin-rotational invariance<sup>20</sup> and  $\langle \dots \rangle_{\text{dis}}$  stands for the disorder average. The staggered magnetization per dopant is then simply  $m_{\text{spin}} = m_{AF}/x$ . We have checked that extrapolations to the thermodynamic limit using different aspect ratios  $L_y/L_x$  give similar results and, here, we only report data for  $L_y = L_x = L$ .

Since, strictly speaking, in 2D the divergence of  $S(\pi, \pi)$  occurs only at  $T = 0$  ( $\beta = \infty$ ) it is appropriate to first extrapolate the finite size numerical data to  $T = 0$ . As shown in Fig. 2 the staggered structure factor saturates at sufficiently low temperature and the GS value of  $m_{AF}$  (averaged over disorder) can be safely obtained. Then, using a polynomial fit in  $1/\sqrt{N_s}$  (order 2 is sufficient) an accurate extrapolation to the thermodynamic limit,  $N_s \rightarrow \infty$  (or  $L \rightarrow \infty$  at constant  $x$ ), is performed as shown in Fig.3(a). The doping dependance of the extrapolated  $m_{AF}$  is given in Fig.3(b). Note that our results, although consistent with previous ( $T = 0$ ) extrapolations attempted on small clusters<sup>11</sup>, are far more accurate due to the use of much larger systems. We have tested various fits to the data. Assuming a power law  $\propto x^\mu$ , the best fit (solid line in Fig.3(b)) gives an exponent  $\mu \simeq 1.38 > 1$ . However, the alternative behavior  $a_1 x + a_2 x^2$  would only be distinguishable at even smaller  $x$ .

We have computed the uniform susceptibility  $\chi(T)$  for

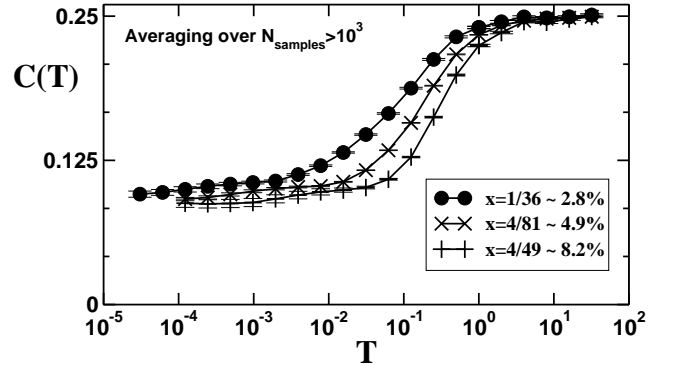


FIG. 4: Curie constant  $\chi \times T$  vs  $T$  shown for  $N_s = 144$  spins and 3 different concentrations  $x$  (as shown on plot).

a wide range of temperatures. Results for the Curie constant  $C(T) = T\chi(T)$  are shown in Fig. 4. At the highest temperatures the effective dopant spins behave as free spins while at low temperature we observe a new Curie-like behavior with a reduced Curie constant  $\sim 1/12$ . Although here the 2D system orders at  $T = 0$  (as proven above) this behavior agrees with a qualitative argument by Sigrist and Furusaki<sup>16</sup> based on the formation of large spin clusters. A detailed analysis of a low-temperature scaling regime similar to the one observed in random ferromagnetic-antiferromagnetic spin chains<sup>21</sup> will be reported elsewhere<sup>23</sup>.

We finish this investigation by calculating the Néel temperature, assuming a small (effective) 3D magnetic coupling  $\lambda_{3D}$  between the 2D planes. Using an RPA criterion, the critical temperature  $T_N$  is simply given by  $\chi_{\text{stag}}(T_N) = 1/|\lambda_{3D}|$  where the staggered spin susceptibility (normalized per site) is defined as usual by,

$$\chi_{\text{stag}}(T) = \frac{1}{L^2} \sum_{i,j} (-1)^{r_i+r_j} \int_0^\beta d\tau \langle S_i^z(0) S_j^z(\tau) \rangle, \quad (6)$$

and averaged over several disorder configurations (typically 2000). Since  $\chi_{\text{stag}}(T_N)$  is expected to reach its thermodynamic limit for a *finite* linear size  $L$  as long as  $T_N$  remains *finite*, accurate values of  $T_N$  can be obtained using a finite size computation of  $\chi_{\text{stag}}(T)$  for not too small inter-chain couplings. Fig. 5(a) shows that  $\chi_{\text{stag}}(T)$  diverges when  $T \rightarrow 0$ .  $T_N$  is determined by the intersection of the curve  $\chi_{\text{stag}}(T)$  with an horizontal line at coordinate  $1/\lambda_{3D}$ . Note that finite size corrections remain small, even in the worst case corresponding to very small  $\lambda_{3D}$  values and large dopant concentrations. The doping dependance of  $T_N$  is plotted in Fig. 5(b) for a particularly small value  $\lambda_{3D} = 0.01$  (in order to show the small size dependance observable in that case). It clearly reveals a rapid decrease of  $T_N$  when  $x \rightarrow 0$ , but, in agreement with experiments, does not suggest a non-zero critical concentration. In Fig.5(b), we show the behavior of  $T_N(x)$  down to  $x \simeq 0.007$ . Note that from numerical fits of our data, we can not clearly distinguish between a power-law be-

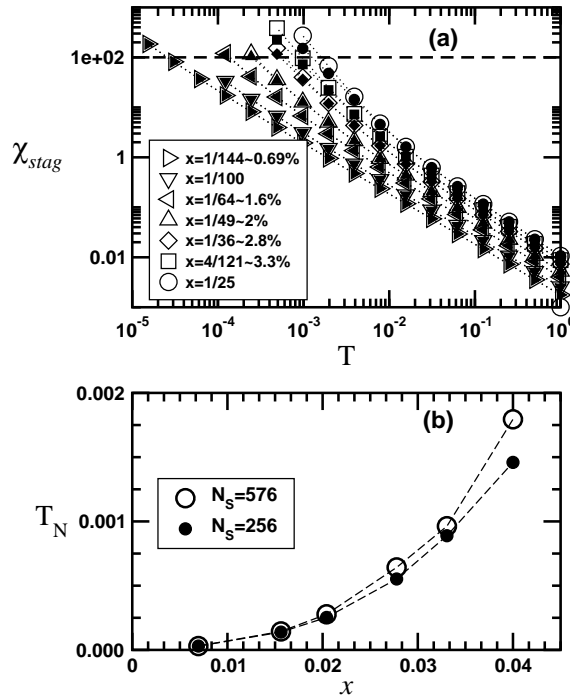


FIG. 5: (a) Staggered susceptibility of a 2D layer vs temperature (using log-log scales) for  $N_s = 256$  (full symbols) and  $N_s = 576$  (open symbols) spins. Concentrations  $x$  are shown on the plot (similar symbols as in Figs. 2 and 3).  $\lambda_{3D}^{-1} = 100$  is shown by the dashed line. (b) Néel temperature vs dopant concentration  $x$  for a 3D RPA inter-plane coupling  $\lambda_{3D} = 0.01$  and for  $N_s = 256$  and  $N_s = 576$  spins.

havior (with an exponent  $\sim 2.5$ ) and an exponential law like  $A \exp(-B/x)$ , as suggested by fits of experimental data for  $\text{Cu}_{1-x}\text{Zn}_x\text{GeO}_3$ <sup>22</sup>.

In summary, we have studied an effective low-energy Hamiltonian (valid for low temperature physics) describing the interaction of a finite concentration of spinless dopants randomly distributed in a generic low-dimensional (frustrated) SP system. The SSE method, which is applicable here because of the non-frustrated nature of the effective model, was used in combination with finite-size scaling to compute both GS and finite temperature properties. The uniform susceptibility exhibits a Curie-like behavior down to very low temperature. We also predict that the AF order develops continuously without any finite critical dopant concentration in agreement with experiment.

AWS acknowledges support from the Academy of Finland, project NO. 26175. D.P. thanks M. Sigrist for pointing out that the uniform susceptibility data could be interpreted as a scaling regime. Further investigations along these lines are under way<sup>23</sup>. We thank IDRIS (Orsay, France) for using their supercomputer facilities.

- <sup>1</sup> M. Hase, I. Terasaki, and K. Uchinokura, Phys. Rev. Lett. **70**, 3651 (1993).
- <sup>2</sup> M. Isobe and Y. Ueda, J. Phys. Soc. Jpn. **65**, 3142 (1996); R. Valenti et al., Phys. Rev. Lett. **86**, 5381 (2001).
- <sup>3</sup> F. Becca, F. Mila and D. Poilblanc, Phys. Rev. Lett. **91**, 067202 (2003).
- <sup>4</sup> M. Hase et al., Phys. Rev. Lett. **71**, 4059 (1993); S.B. Oseroff et al., Phys. Rev. Lett. **74**, 1450 (1995); L.-P. Regnault et al., Europhys. Lett. **32** 579 (1995); T. Masuda et al., Phys. Rev. Lett. **80**, 4566 (1998); B. Grenier et al., Phys. Rev. B **58**, 8202 (1998).
- <sup>5</sup> A. Oosawa, T. Ono, and H. Tanaka, Phys. Rev. B **66**, 020405 (2002).
- <sup>6</sup> E. S. Sørensen, I. Affleck, D. Augier, and D. Poilblanc, Phys. Rev. B. **58**, R14701 (1998).
- <sup>7</sup> G. B. Martins, E. Dagotto and J. Riera, Phys. Rev. B. **54**, 16032 (1996).
- <sup>8</sup> T. Nakamura, Phys. Rev. B **59**, R6589 (1999).
- <sup>9</sup> B. Normand and F. Mila, Phys. Rev. B. **65**, 104411 (2002).
- <sup>10</sup> P. Hansen, D. Augier, J. Riera, and D. Poilblanc, Phys. Rev. B. **59**, 13557 (1999).
- <sup>11</sup> A. Dobry et al., Phys. Rev. B. **60**, 4065 (1999).
- <sup>12</sup> N. Laflorencie and D. Poilblanc, Phys. Rev. Lett. **90**, 157202 (2003).

- <sup>13</sup> Chains with in-phase relative dimerisations are stabilized by an energy  $\propto J_\perp^2/J$  (per bond) w.r.t. the alternate configuration; see T.M.R. Byrnes, M.T. Murphy and O.P. Sushkov, Phys. Rev. B. **60**, 4057 (1999).
- <sup>14</sup> I. Affleck, Proceedings of the NATO ASI: Dynamical properties of Unconventional Magnetic Systems, April 1997, cond-mat/9705127 (unpublished).
- <sup>15</sup> In fact, for the *undoped* system, an *exact* mapping exists assuming  $2J_4/J = J/K_{\text{eff}}$  where  $K_{\text{eff}} = K_{\parallel} - 2|K_{\perp}|$ .
- <sup>16</sup> For related studies of a doped spin ladder with *no frustration* see M. Sigrist and A. Furusaki, J. Phys. Soc. Jpn 65, 2385 (1996).
- <sup>17</sup> A. W. Sandvik, Phys. Rev. B **59**, R14157 (1999).
- <sup>18</sup> A. W. Sandvik, Phys. Rev. E **68**, 056701 (2003).
- <sup>19</sup> A. W. Sandvik, Phys. Rev. B **66**, 024418 (2002).
- <sup>20</sup> J. D. Reger and A. P. Young, Phys. Rev. B **37**, 5978 (1988).
- <sup>21</sup> E. Westerberg, A. Furusaki, M. Sigrist and P.A. Lee, Phys. Rev. Lett. **75**, 4302 (1995); B. Frischmuth and M. Sigrist, Phys. Rev. Lett. **79**, 147 (1997); B. Frischmuth et al., Phys. Rev. B **60**, 3388 (1999).
- <sup>22</sup> K. Manabe et al., Phys. Rev. B **58**, R575 (1998).
- <sup>23</sup> N. Laflorencie, D. Poilblanc, A. Sandvik and M. Sigrist, in preparation.